

NETWORK INFECTION SOURCE IDENTIFICATION UNDER THE SIRI MODEL

Wuhua Hu, Wee Peng Tay, Athul Harilal, and Gaoxi Xiao

School of Electrical and Electronic Engineering, Nanyang Technological University, Singapore

ABSTRACT

We study the problem of identifying a single infection source in a network under the susceptible-infected-recovered-infected (SIRI) model. We describe the infection model via a state-space model, and utilizing a state propagation approach, we derive an algorithm known as the heterogeneous infection spreading source (HISS) estimator, to infer the infection source. The HISS estimator uses the observations of node states at a particular time, where the elapsed time from the start of the infection is unknown. It is able to incorporate side information (if any) of the observed states of a subset of nodes at different times, and of the prior probability of each infected or recovered node to be the infection source. Simulation results suggest that the HISS estimator outperforms the dynamic message passing and Jordan center estimators over a wide range of infection and reinfection rates.

Index Terms— Infection source identification, SIRI model, side information, regular tree, Facebook network

1. INTRODUCTION

Consider an infection, which can be a computer virus, disease or rumor, spreading in a network of nodes. A node is said to be in infected state if it “possesses” that infection [1, 2]. For example, in the case of a rumor spreading in an online social network like Facebook, an infected node is a user who has posted the rumor on his social page in the recent past. A node is in susceptible state if it has never been infected before, or in recovered state if it has recovered from an infection. In the Facebook example, a recovered node corresponds to a user who has removed the rumor post or the post is not within a predefined number of most recent postings of the user. An infection follows a susceptible-infected (SI) model if a susceptible node may become infected if it has infected neighbors, and an infected node stays infected [3]. The infection has a susceptible-infected-recovered (SIR) model if an infected node may recover from an infection but then stays uninfected forever [3], and a susceptible-infected-recovered-infected (SIRI) model if a recovered node may again relapse into an infected state, i.e., it does not require any infected neighbors to reinfect it [4, 5]. In the Facebook example, a user may repost a rumor after he has removed it due to influences external to the Facebook network [6, 7]. The SIRI model reduces to an SI or SIR model if the probability of recovery or reinfection is equal to zero, respectively.

Suppose that after an unknown elapsed amount of time since the start of an infection spreading, we have a snapshot of the states of a subset of the network, and we want to identify the infection source based on this snapshot and the network topology. This is known as the network source identification problem, and has been extensively studied under the SI and SIR models. Various source estimators such as the distance (or rumor) center [1, 2, 8], Jordan center [6, 9, 10], dynamic message passing (DMP) estimator [11, 12], belief propagation

(BP) estimator [12, 13], have been proposed and studied. Each of these estimators seeks to find an approximate maximum likelihood, maximum a posteriori (MAP), or most likely infection path estimator of the true infection source, and may require different levels of a priori information about the spreading process. For example, the distance and Jordan center estimators do not require any knowledge of the infection rates, which are utilized by DMP and BP estimators.

In this paper, we consider identifying a single infection source in a network under the SIRI model, which is more general than the SI and SIR models. The SIRI model is frequently used to describe the transmission of a contagious disease with relapse, such as bovine tuberculosis or human herpes virus, in which recovered individuals may revert back to the infectious class due to reactivation of the latent infection or incomplete treatment [4, 5, 14]. The model is also used as a simplified version of general multi-strain models, where after an initial infection, immunity against one strain only gives partial immunity against a genetically close mutant strain [15]. A further example of SIRI type of infection spreading is rumor spreading in an online social network, as alluded to earlier in the Facebook example. It is thus of both practical and theoretical interest to consider infection spreading and source identification in a network under the SIRI model. However, the problem is more challenging than the one under the SI and SIR models because a node may become infected and recovered multiple times. Therefore, it is unclear if the infection source estimators currently proposed in the literature can be applied directly to the SIRI model, and if this will lead to significant performance deterioration.

In this paper, we aim to find an approximate MAP estimator for inferring the infection source under the SIRI model. Our estimator is derived as a non-trivial extension of the DMP estimator, which cannot be applied directly to the SIRI model because it violates the assumption of unidirectional state transitions [16]. Our estimator is also related to the revised version of DMP called DMP_r in [13], which is also applicable only to the SIR model. Furthermore, our new estimator is able to incorporate side information such as the prior probability of each candidate node being the infection source, and additional observations on subsets of nodes in periods other than the snapshot time. We call our new estimator the heterogeneous infection spreading source (HISS) estimator for its applicability to a network with nodes following different (i.e., SI, SIR and SIRI) infection models. Simulations are performed on random regular tree networks and a subset of Facebook network to evaluate the proposed estimator and compare its performance with those of the Jordan center estimator, and the DMP estimator. Our simulation results suggest that the HISS estimator outperforms both the Jordan center and DMP estimator over a wide range of infection and reinfection rates.

2. INFECTION MODEL AND ASSUMPTIONS

In this section, we characterize the SIRI infection spreading using a state-space approach [17]. Throughout this paper, we assume a

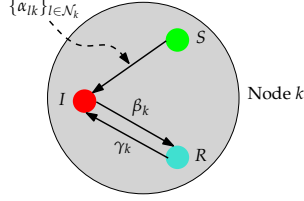


Fig. 1. Possible state transitions of a node under the SIRS model.

common underlying probability space with probability measure \mathbb{P} . We also use $0 : n$ to denote the integer set $\{0, 1, \dots, n\}$.

Let the network over which the infection spreads be described by a directed graph, $(\mathcal{N}, \mathcal{E})$, where $\mathcal{N} \triangleq 1 : N$ is the node set and \mathcal{E} is the edge set. A directed edge (l, k) exists from node l to node k if node l can directly infect node k , in which case node l is said to be an *in-neighbor* of node k , and conversely node k is said to be an *out-neighbor* of node l . We denote the set of in-neighbors of a node k as \mathcal{N}_k .

Suppose that there is a single node s^* in the network that starts the infection at time 0, and suppose that we observe the node states of a set of nodes in the network at a particular time T_f , which we call the *snapshot* time. We assume that T_f is unknown, and that time is discretized into $0 : T_f$. Let S , I , and R denote the susceptible, infected, and recovered states, respectively. Let α_{lk} be the probability of an infected node l infecting an out-neighbor k within a time slot, where $\alpha_{lk} = 0$ if $l \notin \mathcal{N}_k$. Let β_k be the probability of an infected node k to recover within a time slot, and γ_k be the probability of a recovered node k to be infected again within a time slot, where $\gamma_k = 0$ if $\beta_k = 0$. These probabilities are assumed to be given or have been inferred a priori. The possible state transitions of a node are depicted in Fig. 1. It is evident that the infection process at node k reduces to the SIR model if $\gamma_k = 0$, and the SI model if we further have $\beta_k = 0$. This admits a heterogeneous spreading model containing different infection processes of SI, SIR and SIRS at different nodes. Our model thus subsumes those studied in [1, 2, 9, 13, 16]. We assume that conditioned on the node states in time slot $t - 1$, all node transitions in time slot t are independent of each other.

We use $P_k^S(t)$, $P_k^I(t)$ and $P_k^R(t)$ to denote the probabilities of a node $k \in \mathcal{N}$ to be in states S , I and R at time t , respectively. Adopting a state-space modeling approach, we define these three probabilities as state variables. The infection model is then obtained by describing the evolution of the three state variables in time using difference equations. Using the state transitions for the SIRS model, we have for all $t \in 1 : T_f$ and $k \in \mathcal{N}$,

$$P_k^S(t) = \mathbb{P}(\bar{U}_k(t-1) | S_k(t-1)) \cdot P_k^S(t-1), \quad (1)$$

$$P_k^R(t) = \beta_k P_k^I(t-1) + (1 - \gamma_k) P_k^R(t-1), \quad (2)$$

$$P_k^I(t) = 1 - P_k^S(t) - P_k^R(t), \quad (3)$$

where $\bar{U}_k(t-1)$ is the event that no in-neighbor passes the infection to node k in during time $t - 1$ to t , and $S_k(t-1)$ is the event that node k is in state S at time $t - 1$. By assuming that in-neighbors pass infection to a node independently, and utilizing the mean-field approximation, we have

$$\mathbb{P}(\bar{U}_k(t-1) | S_k(t-1)) \approx \prod_{l \in \mathcal{N}_k} (1 - \alpha_{lk} P_l^{I|S_k(t-1)}(t-1)), \quad (4)$$

where $P_l^{I|S_k(t_1)}(t_2) \triangleq \mathbb{P}(I_l(t_2) | S_k(t_1))$, for all $t_1, t_2 \in 0 : T_f$, which is the probability that node l is in state I at time t_2 given that

node k is in state S at time t_1 . (Note that equation (4) is exact if the graph $(\mathcal{N}, \mathcal{E})$ is acyclic.) To complete the model, we need to have an explicit expression for $P_l^{I|S_k(t-1)}(t-1)$.

To that end, we introduce two classes of auxiliary state variables. For all $t \in 0 : T_f$, $l \in \mathcal{N}_k$, $k \in \mathcal{N}$, let $\theta_{lk}(t)$ be the probability of a node l not infecting its out-neighbor k up to time t , given that node k is in state S at time t ; and let $\phi_{lk}(t)$ be the probability of a node l to be in state I at time t and not infecting its out-neighbor k up to time t , given that node k is in state S at time t . Then it can be shown that

$$P_l^{I|S_k(t-1)}(t-1) = \frac{\phi_{lk}(t-1)}{\theta_{lk}(t-1)}, \quad (5)$$

where $\theta_{lk}(t-1)$ and $\phi_{lk}(t-1)$ are updated by

$$\theta_{lk}(t) = \theta_{lk}(t-1) - \alpha_{lk} \phi_{lk}(t-1), \quad (6)$$

$$\begin{aligned} \phi_{lk}(t) = & (1 - \alpha_{lk})(1 - \beta_l) \phi_{lk}(t-1) \\ & + (P_l^{S|S_k(t-1)}(t-1) - P_l^{S|S_k(t)}(t)) \\ & + \gamma_l P_l^{R|S_k(t-1)}(t-1), \end{aligned} \quad (7)$$

and the auxiliary conditional probabilities are computed from

$$P_l^{S|S_k(t-1)}(t-1) = P_l^S(0) \prod_{j \in \mathcal{N}_l \setminus \{k\}} \theta_{jl}(t-1), \quad (8)$$

$$P_l^{R|S_k(t-1)}(t-1) = 1 - P_l^{S|S_k(t-1)}(t-1) - P_l^{I|S_k(t-1)}(t-1). \quad (9)$$

Compared to the DMP equations in [11], the new term at the end of (7) arises from the reinfection of a recovered node, which is unique to the SIRS infection model. This term is then computed by (9), which further depends on the new equation (5) and equation (8). The key equation (5) follows from an important observation:

$$\begin{aligned} P_k^S(t) &= P_k^S(0) \prod_{l \in \mathcal{N}_k} \theta_{lk}(t) = P_k^S(t-1) \prod_{l \in \mathcal{N}_k} \frac{\theta_{lk}(t)}{\theta_{lk}(t-1)} \\ &= P_k^S(t-1) \prod_{l \in \mathcal{N}_k} \left(1 - \alpha_{lk} \frac{\phi_{lk}(t-1)}{\theta_{lk}(t-1)} \right) \\ &= P_k^S(t-1) \prod_{l \in \mathcal{N}_k} \left(1 - \alpha_{lk} P_l^{I|S_k(t-1)}(t-1) \right), \end{aligned}$$

where the last equality follows from (1) and (4). We note that for a directed acyclic graph, the above equations are exact, while we will treat these as approximations for general network graphs.

We proceed to associate *virtual* observation equations with the state dynamics. Let \mathcal{N}_t^S , \mathcal{N}_t^I and \mathcal{N}_t^R denote the sets of nodes observed to be in states S , I and R at time t , respectively; and \mathcal{N}_t^{SIR} denote the set of nodes observed to be in an uninfected state but are indistinguishable to be in state S or R at time t . The rest of the nodes whose states are unknown or not observed are collected into a set denoted by \mathcal{N}_t^{SIR} , i.e., $\mathcal{N}_t^{SIR} = \mathcal{N} \setminus (\mathcal{N}_t^S \cup \mathcal{N}_t^I \cup \mathcal{N}_t^R \cup \mathcal{N}_t^{SIR})$. Stack the three states into a single vector as $P_k(t) \triangleq [P_k^S(t) P_k^I(t) P_k^R(t)]^T$. We define the virtual observations as

$$y_k(t) = C_k(t) P_k(t), \quad (10)$$

where the observation vector $C_k(t) \in \mathbb{R}^{1 \times 3}$ takes one of the feasible values: $[1 \ 0 \ 0]$, if $k \in \mathcal{N}_t^S$; $[0 \ 1 \ 0]$, if $k \in \mathcal{N}_t^I$; $[0 \ 0 \ 1]$, if $k \in \mathcal{N}_t^R$; $[1 \ 0 \ 1]$, if $k \in \mathcal{N}_t^{SIR}$; $[1 \ 1 \ 1]$, if $k \in \mathcal{N}_t^{SIR}$. The last observation vector corresponds to a null observation and is defined merely for theoretical completeness.

3. IDENTIFYING THE INFECTION SOURCE

We assume that at a particular observation snapshot time T_f , we wish to infer the identity of the infection source. For each node k , let W_k be the set of time slots during which the state of node k is observed. The time slots in W_k are known only relative to the unknown snapshot time T_f , which is to be inferred. For each $t \in W_k$, let $X_{k,t} \in \{S, I, R, SR\}$ be the observed state of node k at time t , where SR represents an observation state in which we are unable to distinguish an uninfected state as either S or R . We lump all observation times into a set $\mathcal{T}^O = \cup_{k \in \mathcal{N}} W_k$. Let \mathcal{N}^O be the set of all nodes with at least one observation up to the snapshot time.

We exclude all observed susceptible nodes whose in-neighbors are also observed to be susceptible, because these nodes do not contribute to the infection realization [12]. We use \mathcal{N}' to denote the full node set \mathcal{N} with such uninformative nodes removed, and \mathcal{N}'_k to denote the neighbors of node k in the reduced graph for all $k \in \mathcal{N}'$.

Let \mathcal{N}^c be the set of nodes that have been observed to be in states I , R , or SR at some observation time (i.e., the candidate sources). Moreover, the prior probability of a candidate to be the infection source is denoted by $P_{k,0}^I$ for all $k \in \mathcal{N}^c$.

We formulate the source identification problem as an approximate MAP estimation of the infection source. Ideally, the true infection source and the true snapshot time should be estimated as

$$(\hat{s}, \hat{T}_f) \in \underset{s \in \mathcal{N}^c, T_f \in \mathcal{T}^c}{\operatorname{argmax}} \mathbb{P}(s^* = s, \mathcal{N}^O), \quad (11)$$

where \mathcal{T}^c is the set of candidate snapshot times, and $\mathbb{P}(s^* = s, \mathcal{N}^O)$ is the joint probability of node s being the infection source s^* , and \mathcal{N}^O being the given observations. By Bayes' rule, the ideal estimator is equivalent to maximizing $\mathbb{P}(\mathcal{N}^O | s^* = s) \mathbb{P}(s^* = s)$. For tractability, we approximate the joint probability $\mathbb{P}(\mathcal{N}^O | s^* = s)$ by a mean-field probability $\prod_{k \in \mathcal{N}^O} \prod_{t \in W_k} P_k^{X_{k,t} | I_s(0)}(t)$. As the probabilities $P_k^{X_{k,t} | I_s(0)}(t)$ can be computed by iterating the infection model (1)-(10) for a given infection source s , this mean-field probability can be computed and then used to compare different candidate infection sources. Together with an approximate prior $\mathbb{P}(s^* = s)$, the estimator gives an approximate MAP estimation of the infection source.

Therefore, the inference problem can be written in the following optimization form:

$$\begin{aligned} (P0) \quad & \max_{T_f, \{P_k^I(0)\}_{k \in \mathcal{N}^c}} \sum_{s \in \mathcal{N}^c} P_s^I(0) \prod_{k \in \mathcal{N}^O} \prod_{t \in W_k} y_k(t) \\ & \text{subject to} \quad (1) - (10), \\ & P_k^S(0) = 1 - P_k^I(0), \forall k \in \mathcal{N}^c, \quad (12) \\ & P_k^S(0) = 1, \forall k \in \mathcal{N}' \setminus \mathcal{N}^c, \quad (13) \\ & P_k^I(0) = 0, \forall k \in \mathcal{N}' \setminus \mathcal{N}^c, \quad (14) \\ & P_k^R(0) = 0, \forall k \in \mathcal{N}', \quad (15) \\ & \theta_{lk}(0) = 1, \forall l \in \mathcal{N}'_k, k \in \mathcal{N}', \quad (16) \\ & \phi_{lk}(0) = P_k^I(0), \forall l \in \mathcal{N}'_k, k \in \mathcal{N}', \quad (17) \\ & \sum_{k \in \mathcal{N}^c} P_k^I(0) = 1, \\ & T_f \in \mathcal{T}^c, P_k^I(0) \in \{0, 1\}, \forall k \in \mathcal{N}^c, \end{aligned}$$

where the infection model (1)-(10) is applied to a reduced graph which excludes the aforementioned observed uninformative suscep-

tible nodes, and (12)-(17) specify the initial conditions of the infection model.

Note that the observation variables $y_k(t)$ in the objective function are expressed by state variables $P_k(t)$ via (10), and that the basic state variables $P_k(t)$ and the auxiliary state variables $\theta_{lk}(t)$ and $\phi_{lk}(t)$, for all $t \geq 0$, $l \in \mathcal{N}_k$ and $k \in \mathcal{N}$, are determined by the decision variables $P_k^I(0)$ for all $k \in \mathcal{N}^c$ via (1)-(10). Therefore, the optimization essentially depends on the decision variables $\{P_k^I(0)\}_{k \in \mathcal{N}^c}$ and T_f . We also note that T_f is larger than the elapsed time between the time when the first side information is observed and the snapshot time.

Because of the nonlinearities involved in the infection model (1)-(10), it is difficult to solve (P0) by a standard optimization solver. Nonetheless, it is straightforward to get a solution by enumerating and comparing all feasible solutions of (P0). Given a candidate source and a value of T_f , the algorithmic complexity of computing the objective function is $O(dT_f|\mathcal{N}'|)$, where d is the average in-degree of the reduced graph. Since we need to enumerate all candidate values of T_f for all candidate sources, the overall algorithmic complexity is then $O(dT_f|\mathcal{N}'||\mathcal{N}^c||\mathcal{T}^c|)$.

Our proposed inference process inherits the merit of the DMP method, but it is able to incorporate available side information (if any) and is applicable to a network consisting of nodes that follow heterogeneous (namely, SI, SIR and SIRS) infection models. For this reason, we call this new estimator the HISS estimator for short.

Although the HISS estimator is derived by assuming that the in-neighbors pass infections to a node independently (cf. (4)), we can still apply it heuristically to a network where this assumption is violated. We expect that the impact on the performance of the HISS estimator to be small if the network is sparse or has weak correlations between infections passed by neighboring nodes. We note that a similar argument was used to explain the success of well-known BP methods in general network [18].

4. PERFORMANCE EVALUATION VIA SIMULATIONS

We apply the proposed HISS estimator to infer single infection sources in random regular tree networks and a subset of the Facebook network under the SIRS model, and then compare the inference results with those obtained with the DMP and Jordan centre (JC) estimators. In applying the DMP estimator, we ignore the reinfection probability of a recovered node and hence naively treat the SIRS model as an SIR model. In the simulations, we assume that the snapshot time falls in the range $[\tau + 1, T_f + \tau - 1]$, where T_f is the actual elapsed time and τ is the elapsed time since the first side information is observed till the snapshot observation time. In simulations we set τ to $T_f/2$ if T_f is even and $(T_f - 1)/2$ if T_f is odd. We assume uniform infection, recovery and reinfection rates at all nodes in the network.

To compare the estimators, we adopt the following two metrics, which are correlated to the likelihood of wrongly inferring the source and the absolute inference error in distance, respectively:

- *Normalized rank of s^** [11, 12]: We first rank the candidate sources in descending order according to the objective function value in (P0). The rank (≥ 1) of the true infection source, subtracted by the ideal rank value of 1 (yielding the rank error), and then divided by the total number of candidate sources, gives in the desired normalized rank.
- *Error distance of \hat{s} to s^** [19]: We compute the length of the shortest path from the source estimate \hat{s} to the true source s^* .

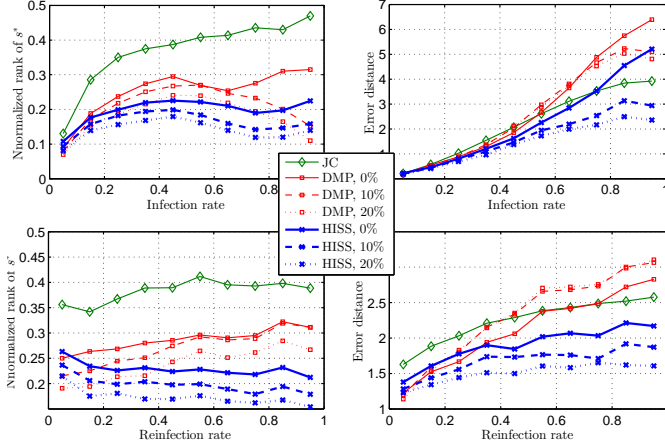


Fig. 2. Comparison of estimators' performance for random regular tree networks. The percentage refers to the fraction of nodes, selected at random at time $T_f - \tau$, whose states are observed.

In the case of regular tree networks, in each instance, we randomly generate a tree network of 1000 nodes with each node's degree equal to 4 [11, 12], and randomly choose an infection source. We then simulate the infection spreading until either 10 time slots or no less than 20% of the nodes are infected or recovered. We observe the states of all nodes at the last simulation time slot. To simulate the availability of different side information, we also collect the states of a random selection of a given percentage (0%, 10% or 20%) of the nodes at time $T_f - \tau$. The inference results, averaged over 1000 random instances, are shown in Fig. 2. As the infection rate increases while the reinfestation rate is fixed at 0.5, we observe that HISS outperforms DMP and JC for most infection rates w.r.t. both performance metrics. We also observe that incorporating additional observations (side information) always improves the performance of HISS. However, this is not always true for DMP since the side information may mislead the inference process due to the spreading model mismatch. As the reinfestation rate increases while the infection rate is fixed at 0.5, we observe that the advantage of HISS over DMP and JC becomes more obvious due to its use of a more general infection model in the inference. Again, incorporating additional observations improves the performance of HISS but may deteriorate that of DMP. The results also show that an estimator that is stronger in one performance metric may be weaker in the other performance metric, which is clear by comparing the performances of DMP and JC.

In the case of the Facebook network, we arbitrarily select a subset of 500 nodes from the Facebook dataset used in [20]. In each simulation instance, we randomly specify an infection source and perform simulations under the same parameter settings as the regular trees. The results are shown in Fig. 3. We observe that, in the absence of side information, HISS outperforms DMP w.r.t. both performance metrics for most infection and reinfestation rates. However, incorporating additional observations does not necessarily improve and may even deteriorate the performance of both HISS and DMP, in which case HISS may become inferior to DMP. This occurs because the Facebook network subset is found to be very loopy and contain many circular subsets, which tends to invalidate the mean-field assumption embedded in the HISS and DMP estimators. Despite this intrinsic limitation, both DMP and HISS outperform JC for almost

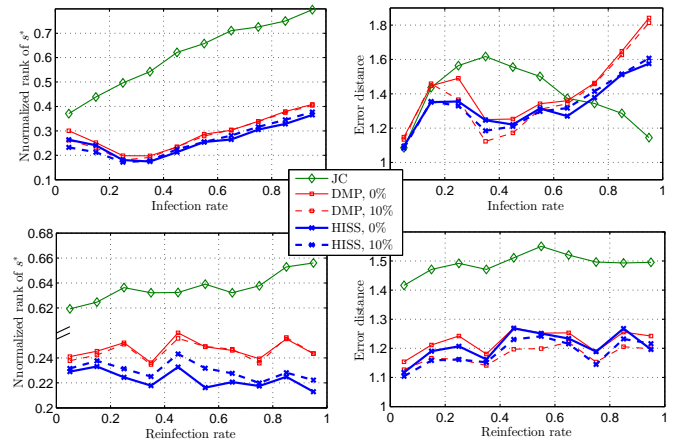


Fig. 3. Comparison of estimators' performance for a subset of the Facebook network. The percentage refers to the fraction of nodes, selected at random at time $T_f - \tau$, whose states are observed.

all infection and reinfestation rates, except when infection rates are high in which case JC has the smallest average error distance. Its corresponding average normalized rank of the true source however remains the largest among the three estimators.

5. CONCLUSION

We have introduced a state-space description of an SIRS infection model, and using the state propagation equations, we have derived an approximate MAP estimator for the infection source, given the observations of a set of node states at a snapshot time. Our proposed estimator is able to incorporate side information like observations of node states at intermediate times during the infection spreading and prior beliefs of potential candidate infection sources, into the inference procedure. Simulations on random regular tree networks and a subset of the Facebook network suggest that the HISS estimator outperforms the Jordan center and DMP estimator for a wide range of the infection and reinfestation rates. However, we note that in networks that are very loopy, adding side information may lead to a performance deterioration. Future work includes designing better inference procedures that can handle side information better for loopy networks.

6. ACKNOWLEDGMENT

The authors are grateful to Andrey Y. Lokhov for sharing with us the DMP implementation code which helped us in implementing the HISS method and doing the comparisons. The authors also thank Wugong Luo for helpful discussions. The research is supported in part by the Singapore Ministry of Education Academic Research Fund Tier 2 grant MOE2013-T2-2-006.

7. REFERENCES

- [1] D. Shah and T. Zaman, "Rumors in a network: Who's the culprit?" *IEEE Trans. Inf. Theory*, vol. 57, no. 8, pp. 5163–5181, 2011.

- [2] W. Luo, W. P. Tay, and M. Leng, "Identifying infection sources and regions in large networks," *IEEE Trans. Signal Process.*, vol. 61, no. 11, pp. 2850–2865, 2013.
- [3] M. J. Keeling and K. T. Eames, "Networks and epidemic models," *Journal of the Royal Society Interface*, vol. 2, no. 4, pp. 295–307, 2005.
- [4] D. Tudor, "A deterministic model for herpes infections in human and animal populations," *SIAM Review*, vol. 32, no. 1, pp. 136–139, 1990.
- [5] P. Van den Driessche and X. Zou, "Modeling relapse in infectious diseases," *Mathematical Biosciences*, vol. 207, no. 1, pp. 89–103, 2007.
- [6] W. Luo, W. Tay, and M. Leng, "How to identify an infection source with limited observations," *IEEE J. Sel. Topics Signal Process.*, vol. 8, no. 4, pp. 586 – 597, 2014.
- [7] W. Luo and W. P. Tay, "Finding an infection source under the SIS model," in *Proc. IEEE 38th International Conference on Acoustics, Speech, and Signal Processing (ICASSP)*, 2013.
- [8] W. Dong, W. Zhang, and C. W. Tan, "Rooting out the rumor culprit from suspects," in *2013 IEEE International Symposium on Information Theory Proceedings (ISIT)*, Istanbul, Turkey, 2013, pp. 2671–2675.
- [9] K. Zhu and L. Ying, "Information source detection in the sir model: a sample path based approach," in *Information Theory and Applications Workshop (ITA), 2013*, 2013, pp. 1–9.
- [10] —, "A robust information source estimator with sparse observations," *To appear in Computational Social Networks*, *arXiv preprint arXiv:1309.4846*, 2014.
- [11] A. Y. Lokhov, M. Mézard, H. Ohta, and L. Zdeborová, "Inferring the origin of an epidemic with dynamic message-passing algorithm," *Phys. Rev. E*, vol. 9, no. 012801, 2014.
- [12] F. Altarelli, A. Braunstein, L. Dall'Asta, A. Lage-Castellanos, and R. Zecchina, "Bayesian inference of epidemics on networks via belief propagation," *Phys. Rev. Letts.*, vol. 112, no. 11, p. 118701, 2014.
- [13] F. Altarelli, A. Braunstein, L. Dall'Asta, A. Ingrosso, and R. Zecchina, "The zero-patient problem with noisy observations," *arXiv preprint arXiv:1408.0907*, 2014.
- [14] P. Guo, X. Yang, and Z. Yang, "Dynamical behaviors of an siri epidemic model with nonlinear incidence and latent period," *Advances in Difference Equations*, vol. 2014, no. 1, p. 164, 2014.
- [15] J. Martins, A. Pinto, and N. Stollenwerk, "A scaling analysis in the siri epidemiological model," *Journal of Biological Dynamics*, vol. 3, no. 5, pp. 479–496, 2009.
- [16] A. Y. Lokhov, M. Mézard, and L. Zdeborová, "Dynamic message-passing equations for models with unidirectional dynamics," *arXiv preprint arXiv:1407.1255*, 2014.
- [17] C. T. Chen, *Linear System Theory and Design*. Oxford: Oxford University Press, 1999.
- [18] K. P. Murphy, Y. Weiss, and M. I. Jordan, "Loopy belief propagation for approximate inference: An empirical study," in *Proceedings of the Fifteenth Conference on Uncertainty in Artificial Intelligence*. Morgan Kaufmann Publishers Inc., 1999, pp. 467–475.
- [19] W. Luo, "Identifying infection sources in a network," Ph.D. dissertation, Nanyang Technological University, Singapore, Aug 2014.
- [20] J. Leskovec and J. J. Mcauley, "Learning to discover social circles in ego networks," in *Advances in Neural Information Processing Systems 25*, 2012, pp. 539–547.